HHS Public Access

Author manuscript

Biochemistry. Author manuscript; available in PMC 2020 February 13.

Published in final edited form as:

Biochemistry. 2019 April 30; 58(17): 2260–2268. doi:10.1021/acs.biochem.8b00939.

Isatins Inhibit N^5-CAIR Synthetase by a Substrate Depletion Mechanism

Cale C. Streeter, **Qian Lin**, **Steven M. Firestine***

Department of Pharmaceutical Sciences, Eugene Applebaum College of Pharmacy and Health Sciences, Wayne State University, Detroit, Michigan 48201, United States

Abstract

The continued rise of antibiotic-resistant infections coupled with the limited pipeline of new antimicrobials highlights the pressing need for the development of new antibacterial agents. One potential pathway for new agents is *de novo* purine biosynthesis as studies have shown that bacteria and lower eukaryotes synthesize purines differently than humans. Microorganisms utilize two enzymes, N^5-CAIR synthetase and N^5-CAIR mutase, to convert 5-aminoimidazole ribonucleotide (AIR) into 4-carboxy-5-aminoimidazole ribonucleotide (CAIR) through the intermediate N^5-carboxy-5-aminoimidazole ribonucleotide (N^5-CAIR). In contrast, vertebrates directly convert AIR to CAIR via the enzyme AIR carboxylase. A high-throughput screen against N^5-CAIR synthetase identified a group of compounds with a 2,3-indolinedione (isatin) core that inhibited the enzyme. While initial studies suggested that isatins inhibited the enzyme by a noncompetitive mechanism, here we show that isatins inhibit N^5-CAIR synthetase by a substrate depletion mechanism. Unexpectedly, we found that isatin reacts rapidly and reversibly with the substrate AIR. The rate of the reaction is dependent upon the substituents on the phenyl moiety of isatin, with 5- and 7-bromoisatin being faster than 4-bromoisatin. These studies suggest that care should be taken when exploring isatin compounds because the biological activity could be a result of their reactivity.

Graphical Abstract

According to the Centers for Disease Control and Prevention, the rise of antibiotic-resistant infections constitutes a critical public health threat that must be addressed. One way to accomplish this is to discover antibiotics that target pathways not currently exploited by existing antimicrobial agents.[1] One possible target is the *de novo* purine biosynthetic

*Corresponding Author sfirestine@wayne.edu. Phone: 1-313-577-0455. Fax: 1-313-577-2033.

ASSOCIATED CONTENT

Accession Codes

N^5-CAIR synthetase (*E. coli*), P09029; N^5-CAIR synthetase (*A. clavatus*, residues 1–383), A1CII2; N^5-CAIR mutase (*E. coli*), P0AG19; SAICAR synthetase (*E. coli*), P0A7D7.

The authors declare no competing financial interest.

pathway. This pathway converts phosphoribosyl pyrophosphate (PRPP) to inosine monophosphate (IMP) in all organisms. Research in the 1990s showed that microbes require 11 enzymatic steps to accomplish this transformation while humans utilize 10.[2,3] The divergence in the pathway occurs for the conversion of 5-aminoimidazole ribonucleotide (AIR) to 4-carboxy-5-aminoimidazole ribonucleotide (CAIR) (Figure 1). Microorganisms convert AIR to the unstable intermediate N^5-carboxy-5aminoimidazole ribonucleotide (N^5-CAIR) using the enzyme N^5-CAIR synthetase.[4] N^5-CAIR is then converted to CAIR via N^5-CAIR mutase.[5] Direct carboxylation of AIR by the enzyme AIR carboxylase produces CAIR in humans.[6]

The two unique enzymes found in bacterial *de novo* purine biosynthesis provide a biochemical rationale for targeting purine biosynthesis in antibacterial drug design. Additionally, microbes deficient in N^5-CAIR synthetase and mutase are less virulent in animal models of infection.[7–12] Targeting N^5-CAIR mutase represents a significant drug design challenge because it is evolutionarily and structurally related to AIR carboxylase, the enzyme found in humans. Thus, our lab initially focused on identifying inhibitors of N^5-CAIR synthetase. We conducted a high-throughput screen of 48000 compounds against the synthetase.[13] This screen identified 14 compounds, six of which contained an indenedione core that decomposed in water to ninhydrin and were shown to be substrate-reactive. However, another six compounds contained an indole-2,3-dione core, also called isatin, exhibiting IC_{50} values between 11 and 70 μM toward *Escherichia coli* N^5-CAIR synthetase. Michaelis–Menten kinetic analysis of the most potent compound demonstrated noncompetitive kinetics, suggesting that isatins bind to a unique site on the enzyme. To better understand the mechanism of action of these compounds, a series of experiments were performed to elucidate the structure–activity relationship of isatin inhibition of N^5-CAIR synthetase. In this paper, we discuss our findings that demonstrate that isatins do not bind to N^5-CAIR synthetase but instead inhibit the enzyme via substrate depletion. The kinetic profile is substantially different from those of our previous studies on other substrate-reactive synthetase inhibitors. Additionally, this result highlights the necessity for careful analysis of the mechanism of action of compounds identified from high-throughput screens and demonstrates the potentially facile reaction of isatins in aqueous environments.

METHODS

Reagents and Equipment.

Ampicillin sodium salt, $MgCl_2$, B-PER (Pierce Biotechnologies), and Amicon Ultra centrifugal filters were purchased from Fisher Scientific. IPTG (isopropyl β-D-1-thiogalactopyranoside) and HisPur Cobalt resin were purchased from Gold Biotechnology. KCl, ATP, PEP (phosphenolpyruvate), PK/LDH (pyruvate kinase/lactate dehydrogenase), and streptomycin sulfate were purchased from Sigma-Aldrich. NADH, $NaHCO_3$, 1-methylisatin, and 5-bromoisatin were purchased from Acros. The malachite green phosphate assay was purchased from Bioassay Systems. Aspartic acid was purchased from Gibco Laboratories. 4-Bromoisatin was purchased from Matrix Scientific. 7-Bromoisatin was purchased from Alfa Aesar. N^5-CAIR synthetase (*E. coli* and *Aspergillus clavatus*, residues 1–383), N^5-CAIR mutase (*E. coli*), and SAICAR synthetase (*E. coli*) were expressed as His-

tagged proteins as previously described[13–15] and purified via a cobalt column per the manufacturer's instructions. The protein was determined to be >95% pure based on sodium dodecyl sulfate–polyacrylamide gel electrophoresis analysis. AIR was prepared as previously described.[13] The stock AIR concentration was determined by measuring the absorbance at 250 nm in 100 mM Tris (pH 8.0) and using an extinction coefficient of 3270 M^{-1} cm^{-1}.[16] The amount of functional AIR was determined using the SAICAR coupled assay and was determined to be 40% of the ultraviolet–visible (UV–vis) absorbance-determined value. A Synergy2 plate reader by BioTek was used for UV–vis absorbance experiments performed in Corning 96-well UV transparent flat bottom plates. A 1-Bio Cary UV–vis spectrophotometer from Varian was used for UV–vis measurements in 1 mL cuvettes. For the synthesis of isoAIR, all reactions were performed under argon. Solvents were purchased from Acros and used without further purification. Reactions were monitored by thin layer chromatography (TLC) (w/UV at 254 nm) and visualized by UV (254 nm). Column chromatography was carried out with silica gel (40–60 μm). ^{1}H nuclear magnetic resonance (NMR) was recorded on a Varian 600 MHz NMR spectrometer. Chemical shifts are given in parts per million (δ) using tetramethylsilane (TMS) as an internal standard. Mass spectra were recorded with a Micromass LCT Premier XE instrument (Waters) with ESI/TOF.

N^5-CAIR Synthetase ATP-NADH Coupled Assay.

In a 1 mL cuvette, the following components were added to obtain the listed final concentrations: 50 mM HEPES, pH 7.5 buffer containing 20 mM KCl and 6.0 mM $MgCl_2$, 1.1 mM ATP, 0.2 mM NADH, 2.0 mM PEP, 1.0 mM $NaHCO_3$, 5 units of pyruvate kinase/lactate dehydrogenase, 200 μM isatin compounds, 25 μM AIR, and N^5-CAIR synthetase (70 ng of *A. clavatus* or 110 ng of *E. coli*). The reaction was initiated by the addition of the enzyme or the substrate, and the mixture was maintained at room temperature. NADH oxidation was monitored at 340 nm, and the initial velocity of each reaction was determined during the first minute. The data in Figure 2 were fit using smooth curve fit in Kaleidagraph software.

IsoAIR Competition Assay.

The N^5-CAIR synthetase coupled assay was conducted with the following modifications. 1-Methylisatin (200 μM) was incubated with isoAIR (200, 400, or 800 μM) for 2 min. The reaction was initiated by the addition of 70 ng of *A. clavatus* N^5-CAIR synthetase, and the reaction was monitored at 340 nm.

SAICAR Synthetase Coupled Assay.

In a 1 mL cuvette, the following components were added to obtain the listed final concentrations: 50 mM HEPES, pH 7.5 buffer containing 20 mM KCl and 6.0 mM $MgCl_2$, 220 μM ATP, 0.2 mM NADH, 2.0 mM PEP, 1.0 mM $NaHCO_3$, 5 units of pyruvate kinase/lactate dehydrogenase, 10 mM aspartic acid, 1.1 μg of *E. coli* N^5-CAIR synthetase, 7 μg of *E. coli* N^5-CAIR mutase, and 7 μg of *E. coli* SAICAR synthetase. To the reaction mixture were added 1-methylisatin (200 μM) and AIR (50 μM) followed by the initiation of the reaction by the addition of N^5-CAIR synthetase. The reaction was performed at room temperature. The reaction was monitored at 282 nm to determine the concentration of

SAICAR.[17] The amount of SAICAR produced was determined by measuring the change in absorbance at 282 nm using an extinction coefficient of 8480 M^{-1} cm^{-1}.

Reversibility of the AIR:Isatin Product.

The reversibility of the product of 1-methylisatin and AIR was determined using the SAICAR synthetase assay with modifications as described. In a 1 mL cuvette, the following components were added to obtain the listed final concentrations: 50 mM HEPES, pH 7.5 buffer containing 20 mM KCl and 6.0 mM $MgCl_2$, 220 μM ATP, 0.2 mM NADH, 2.0 mM PEP, 1.0 mM $NaHCO_3$, 5 units of pyruvate kinase/lactate dehydrogenase, 10 mM aspartic acid, 1.1 μg of *E. coli* N^5-CAIR synthetase, 7 μg of *E. coli* N^5-CAIR mutase, and 7 μg of *E. coli* SAICAR synthetase. To monitor the production of isatin, 500 μM 1-methylisatin was incubated with 1200 μM AIR for 30 min in buffer. To this were added N^5-CAIR synthetase (1.1 μg), N^5-CAIR mutase (7 μg), and SAICAR synthetase (7 μg) to initiate the reaction, and the progress of 1-methylisatin formation was monitored at 420 nm. The production of AIR from the reversal of the AIR:isatin complex was measured on the basis of the production of SAICAR from AIR. Fifty micromolar AIR was incubated with or without 200 μM 1-methylisatin for 30 min to reach equilibrium. To this were added the remaining materials from the SAICAR synthetase assay, added and the amount of SAICAR produced was monitored at 282 nm. The concentration of SAICAR was determined as described above.

Substrate Depletion Analysis.

The N^5-CAIR synthetase ATP-NADH coupled assay was conducted as noted above scaled to a total volume of 200 μL, and the assay was conducted in a 96-well UV plate. For the assay, seven different concentrations of AIR were used (10, 20, 40, 80, 120, 160, and 200 μM). For each AIR concentration, a range of 7-bromoisatin concentrations were selected such that the relationship between inhibitor and fractional inhibition, μ [$\mu = i/(1 - i)$, where i is the concentration of the inhibitor], was linear. The data were analyzed according to the method of Reiner outlined here.[18]

Two potential mechanisms of inhibition are considered for a reaction between a potential inhibitor and a substrate (Scheme 1). In the first, the reaction of a substrate with an inhibitor results in removal of substrate, and thus, the observed inhibition is due to depletion of the substrate available for the enzyme. In the second, reaction with the inhibitor depletes the substrate but the SI complex itself is also an inhibitor. Reiner derived equations that described the relationship between the total inhibitor concentration (I_t) and μ for each mechanism (eqs 1 and 4). When μ is large (as i approaches 1), these equations simplify to linear equations.

For substrate depletion, eq 1 simplifies to the linear eq 2 with a slope (y_2) of $K_3(1 + S_t/K_1)$. A plot of y_2 versus S_t will be linear according to eq 3. For the mixed mechanism in which substrate depletion and inhibition by the SI complex occur, eq 4 simplified to eq 5. The slope (y_2) of eq 5 is more complex, $K_3K_4(1 + S_t/K_1)/(S_t + K_4)$, and thus, a plot of y_2 versus S_t is nonlinear. Therefore, the relationship of y_2 to S_t is linear for a substrate depletion mechanism and exhibits curvature toward a constant for a substrate–inhibitor complex that inhibits the enzyme.

$$I_t = \left(1 + \frac{S_t}{K_1}\right)\left[\mu K_3 + \frac{\mu S_t}{\mu\left(1 + \frac{S_t}{K_1}\right) + 1}\right] \quad (1)$$

$$I_t = \left(1 + \frac{S_t}{K_1}\right)K_3\mu + \text{int} \quad (2)$$

$$y_2 = \frac{K_3}{K_1}S_t + K_3 \quad (3)$$

$$I_t = \mu K_4\left(1 + \frac{S_t}{K_1}\right)\left(\frac{K_3}{S_t + K_4} + \frac{S_t}{S_t + K_4\left\{1 + \left[1 + \left(\frac{S_t}{K_1}\right)\right]\mu\right\}}\right) \quad (4)$$

$$I_t = \frac{K_3K_4\left(1 + \frac{S_t}{K_i}\right)}{S_t + K_4}\mu + \text{int} \quad (5)$$

$$y_2 = \frac{K_3K_4\left(1 + \frac{S_t}{K_1}\right)}{S_t + K_4} \quad (6)$$

Synthesis of IsoAIR.

5-Amino-1-(5′-O-tert-butyldimethylsilyl-2′,3′-O-isopropylidene-β-D-ribofuranosyl)imidazole-4-carboxamide (2).[19]—To a solution of **1** (1.23 g, 1.86 mmol)[20–22] in anhydrous DMF (25 mL) was added dropwise ethylenediamine (6 mL, 90 mmol) (Scheme 2). The solution turned scarlet after the addition. The reaction mixture was warmed to 50 °C for 4 h, and the solvent was removed *in vacuo*. Column chromatography (2 to 5% MeOH/CH_2Cl_2) gave **2** (0.52 g, 1.27 mmol, 68% yield) as a white solid: TLC (5% MeOH/CH_2Cl_2) R_f = 0.39; ^{1}H NMR (600 MHz, $CHCl_3$) δ 7.03 (s, 1H), 5.60 (d, J = 3.7 Hz, 1H), 5.48 (s, 2H), 4.97 (dd, J = 3.7, 6.8 Hz, 1H), 4.92 (dd, J = 3.8, 6.8 Hz, 1H), 4.19 (dt, J = 2.1, 4.1 Hz, 1H), 3.96 (dd, J = 2.2, 11.5 Hz, 1H), 3.86 (dd, J = 2.0, 11.5 Hz, 1H), 1.59 (s, 3H), 1.37 (s, 3H), 0.92 (s, 9H), 0.12 (s, 3H), 0.11 (s, 3H).[23]

5-Amino-1-(2′,3′-O-isopropylidene-β-D-ribofuranosyl)imidazole-4-carboxylate (3).[24]—A solution of **2** (390 mg, 0.94 mmol) in 6 N NaOH (3 mL) was refluxed for 5 h and then concentrated to dryness *in vacuo*. To the residue was added MeOH (3 × 3 mL), and the remaining solid was removed by filtration. The combined methanol layers were dried *in*

vacuo, and the resulting residue was dissolved in water (100 mL, pH 10). The solution was applied to a 10 mL DEAE cellulose column (HCO_3^- form). The column was washed with water followed by a gradient from 0 to 200 mM NH_4HCO_3. The appropriate fractions containing the desired product were combined and dried by lyophilization three times to remove excess salt to give **3** as a pale yellow solid (238 mg, 0.79 mmol, 83% yield): ^{1}H NMR (600 MHz, D_2O) δ 7.53 (s, 1H), 5.88 (d, J = 3.3 Hz, 1H), 5.31 (dd, J = 3.3, 6.5 Hz, 1H), 5.03 (dd, J = 3.3, 6.4 Hz, 1H), 4.38 (q, J = 3.8 Hz, 1H), 3.75 (dd, J = 3.8, 12.5 Hz, 1H), 3.71 (dd, J = 4.5, 12.4 Hz, 1H), 1.62 (s, 3H), 1.42 (s, 3H); ES-MS [M – 1] found 298.1046, calcd for $C_{12}H_{16}N_3O_6$ 298.1045.

IsoAIR [5-amino-1-(2′,3′-O-isopropylidene-β-D-ribofuranosyl)imidazole] (4).[24] —A solution of **4** (586 mg, 1.96 mmol) in ammonium acetate buffer (10 mL, 20 mM, pH 4.8) was stirred at room temperature for 7 h under argon. The reaction mixture was dried by lyophilization, and the residue was purified by fast column chromatography utilizing 40–60 μm (micrometer, particle size) silica (94/5/1 to 78/20/2 MeOH/CH_2Cl_2/NH_4OH) to give **4** (350 mg, 1.37 mmol, 70% yield) as a yellow solid that turned brown during storage at 20 °C: TLC (89/10/1 MeOH/CH_2Cl_2/NH_4OH) R_f = 0.25; ^{1}H NMR (600 MHz, D_2O) δ 7.57 (s, 1H), 6.44 (s, 1H), 5.89 (d, J = 3.2 Hz, 1H), 5.29 (dd, J = 3.1, 6.4 Hz, 1H), 5.01 (dd, J = 3.3, 6.6 Hz, 1H), 4.33 (q, J = 4.0 Hz, 1H), 3.72 (dd, J = 4.0, 12.6 Hz, 1H), 3.66 (dd, J = 5.1, 12.4 Hz, 1H), 1.63 (s, 3H), 1.42 (s, 3H).[25]

RESULTS

Inhibition Kinetics of Substituted Isatins.

As part of our initial studies to improve inhibition of *E. coli* N^5-CAIR synthetase by isatin analogues, we previously examined the inhibitory activity of a variety of substituted isatins utilizing the same discontinuous phosphate assay as the high-throughput screen. These studies revealed that electron-withdrawing groups on C5 and/or C7 of isatin resulted in more potent inhibitors, while substitutions on C4 and C6 gave worse inhibitors (data not shown). As a follow-up to these studies, we examined the kinetics of inhibition of substituted isatins using a continuous assay in which ADP production was coupled to the conversion of NADH to NAD^+. During these studies, we observed that the order of addition exhibited a profound effect on the kinetics of the inhibitors. When the coupled assay was initiated by the addition of enzyme, a straight line was observed in the assay. However, when the reaction was initiated by the addition of substrate, a different kinetic profile emerged. As shown in Figure 2, curvature was observed for some but not all monosubstituted 4-, 5-, and 7-bromoisatins. The observed curvature was independent of the enzyme source (*A. clavatus* or *E. coli*, 29% identical), indicating that the unique kinetics were not due to a property of the enzyme. The degree of curvature and the time to reach a steady-state rate were dependent upon the site of substitution. 4-Bromoisatin demonstrated weak inhibition and a slight curvature, while 5- or 7-bromoisatin revealed stronger inhibition and more curvature.

The curvature of the kinetic data suggests a time-dependent inhibition of N^5-CAIR synthetase. Time-dependent inhibition could have a variety of mechanistic possibilities, including (1) modification of the inhibitor, (2) reaction of the inhibitor with the enzyme, (3)

reaction of the inhibitor with the substrate, and (4) a slow conformational change of the enzyme. To determine if the time dependence was due to reaction with the substrate or enzyme, preincubation studies were conducted. Incubation of 1-methylisatin with the *A. clavatus* enzyme for 5 min followed by the addition of AIR resulted in curvature. However, incubation of 1-methylisatin with AIR for 5 min followed by the addition of the enzyme resulted in a straight line (Figure 3). These results suggest that the observed curvature is due to a reaction between AIR and isatin. The steady-state slopes for both experiments were comparable, suggesting that in both cases the same concentration of the AIR:isatin complex was eventually formed.

To verify the proposed reaction between AIR and isatin, a competition experiment was conducted using the AIR analogue, isoAIR (Figure 4). IsoAIR has an isopropylidene protecting group on the 2′- and 3′-hydroxyl groups and no 5′-phosphate. Studies indicated that isoAIR is not a substrate or an inhibitor of *A. clavatus* N^5-CAIR synthetase (data not shown). Addition of increasing concentrations of isoAIR reverses the inhibitory effect of isatin (Figure 4). The most likely explanation for this observation is that the excess isoAIR reacts with isatin, preventing a reaction between AIR and isatin. Therefore, AIR remains available as a substrate for the enzymatic reaction.

Reaction of AIR and Isatin Is Reversible.

The observation that isatin reacts with AIR was unexpected as the observed kinetics were completely different from those of a previously identified substrate-reactive molecule.[13] In our HTS efforts, a series of compounds that were converted to ninhydrin in aqueous solution and reacted with AIR were identified. The Michaelis–Menten plots showed that the presence of a slight excess of the ninhydrin analogues resulted in complete consumption of the substrate and 100% inhibition of enzymatic activity. Addition of a slight excess of AIR restored enzymatic activity. In contrast, the isatin analogues never achieved 100% inhibition, even when isatin concentrations were 8-fold greater than AIR concentrations. There are two possible explanations for this observation. First, the observed activity, as measured by conversion of NADH to NAD^+ in the coupled assay, is due to the ATPase activity of N^5-CAIR synthetase. While N^5-CAIR synthetase does exhibit ATPase activity, the rate is approximately 500 times slower than that observed in the presence of isatin, indicating that this explanation is not supported.

Alternatively, the proposed reaction between AIR and isatin could be reversible. As the enzyme consumes AIR, the equilibrium of the AIR:isatin complex is shifted to supply AIR. In addition, AIR is also produced by the non-enzymatic decarboxylation of N^5-CAIR. An increasing concentration of 1-methylisatin results in a more pronounced curvature, and the steady-state enzymatic activity is decreased (Figure 5A), which is consistent with a shift in the equilibrium with an increase in isatin concentration. To further assess the reversibility of the AIR:isatin complex, the reaction must proceed beyond the reversible intermediates, N^5-CAIR and CAIR, to a stable product. To accomplish this, *E. coli* N^5-CAIR synthetase was coupled to *E. coli* N^5-CAIR mutase and *E. coli* SAICAR synthetase (Scheme 3) to produce the nonreversible product phosphoribosylaminoimidazole succinocarboxamide (SAICAR).

Two experiments were independently performed to examine the recovery of the starting materials, isatin and AIR. First, to examine the recovery of isatin, a characteristic absorbance peak at 420 nm for isatin analogues was measured. As shown in Figure 5B, the reaction of isatin and AIR results in a decrease in absorbance at 420 nm as the product is formed. Conversely, when the AIR:isatin product reverts to starting materials, the absorbance peak reappears. To minimize free isatin in these experiments and the associated absorbance at 420 nm, 500 μM 1-methylisatin was incubated with excess AIR (1.2 mM) for 30 min to generate the AIR:isatin complex. Then, the SAICAR coupled assay was initiated by addition of all enzymes required for SAICAR production. As SAICAR was produced, AIR was consumed and the production of the original starting material, 1-methylisatin, was confirmed as the absorbance at 420 nm increased (Figure 6A). Second, to examine the recovery of AIR, the production of SAICAR was measured as an indirect measurement of AIR. In this experiment, 200 μM 1-methylisatin was incubated with 50 μM AIR and the SAICAR synthetase coupled reaction was monitored at 282 nm to show the production of SAICAR. More than 95% of the expected SAICAR was produced after 60 min (Figure 6B), indicating the complete reversibility of the AIR:isatin complex. As expected, the production of SAICAR from the AIR:isatin product is substantially slower than from AIR alone, suggesting that the rate of the reverse reaction is slow.

Isatin Inhibits N^5-CAIR Synthetase via Substrate Depletion.

While these results provide evidence that AIR reacts with isatin, this does not exclude the potential that the AIR:isatin product is an N^5-CAIR synthetase inhibitor. The methodology proposed by Reiner to differentiate inhibition via substrate depletion and inhibition from the substrate:inhibitor (SI) complex was utilized (see Methods for details).[18] In the Reiner methodology, a series of experiments are conducted to determine the fractional inhibition, μ, at various inhibitor and substrate concentrations. The total concentration of inhibitor, I_t, is plotted against the fractional inhibition, μ. The slopes of the resulting linear lines are replotted against the substrate concentrations. A linear replot indicates enzyme inhibition is due to substrate depletion, whereas a curvature in the replot indicates inhibition is a combination of substrate depletion and inhibition of the enzyme by the substrate:inhibitor complex. For these experiments, the potent inhibitor 7-bromoisatin was utilized. The experiments were conducted with seven different AIR concentrations (10–200 μM) and 14 different 7-bromoisatin concentrations (6.25–400 μM), and the fractional inhibition was plotted against the concentration of 7-bromoisatin for each concentration of AIR (Figure 7A). The replot of slopes versus substrate concentration was linear with an R^2 of 0.997 (Figure 7B), suggesting isatin inhibits N^5-CAIR synthetase via pure substrate depletion and not via binding to the enzyme. One characteristic of the replot of the slope versus substrate concentration is that the y-intercept represents the equilibrium constant among the substrate (AIR), the inhibitor (7-bromoisatin), and the substrate:inhibitor complex. The equilibrium constant was calculated to be 1.6 ± 2.5 μM, so the upper value of the equilibrium constant is 4.1 μM. Equilibrium constants cannot be negative values, and we know that the value must be greater than 0 because a reaction between isatin and AIR occurs. Given this, we can estimate the range for the equilibrium constant to be 1.6–4.1 μM. This result was compared to the steady-state inhibitory rate of 100 μM 7-bromoisatin with 25 μM AIR. On the basis of the estimated equilibrium constant, the amount of free AIR expected is 0.5–1.3 μM. This

corresponds to an enzymatic activity of 0.0014–0.0034 OD/min, which is comparable to the actual activity of 0.0024 OD/min measured in the assay.

DISCUSSION

Our previous characterization of isatin analogues as inhibitors of N^5-CAIR synthetase indicated that these compounds were noncompetitive inhibitors of the enzyme. As demonstrated in this paper, that observation was incorrect, and instead, isatins inhibit N^5-CAIR synthetase via substrate depletion. Our results highlight the importance of not relying upon a discontinuous assay for the analysis of inhibitors and the need to validate kinetics with various reaction conditions. From previous work, the phosphate assay and the ATP-NADH coupled assay provide similar results for determining N^5-CAIR synthetase inhibition. However, due to the limitations of the discontinuous phosphate assay and the reaction conditions of the ATP-NADH coupled assay used to assess the type of inhibition by isatins, the time-dependent nature of the inhibition was masked. Previously, the ATP-NADH coupled assay was performed by allowing the reaction mixture to equilibrate to 37 °C and then initiated by addition of enzyme. On the basis of the investigation presented here, it is most likely that during the equilibration period the AIR:isatin complex was formed, resulting in a linear rate of activity upon initiation with enzyme. Such a result indicates that the reactivity of isatins is rapid in an aqueous environment and thus more facile under assay conditions than, perhaps, anticipated.

The reaction between isatin and AIR is surprising given the fact that the kinetics are distinct from those of previously observed AIR-reactive molecules and the fact that the reported isatin reactivity with aromatic amines is poor.[26] An analysis of the PubChem database indicates that isatins have not been identified as promiscuous inhibitors. Reports regarding isatin-like compounds as PAINS (pan-assay interference compounds) have produced differing results. In 2010, interrogation of a series of HTS-campaigns found isatin substructures associated with problematic compounds and could be a component of PAINS.[27] In contrast, two other reports identified the 1-imineisatin substructure as a moderate risk of promiscuity and a nonfrequent hitter.[28,29] Isatins have been shown to react with the sulfhydryl groups in cysteine residues, and isatin analogues inhibit cysteine protease caspase-3 through formation of a covalent bond.[30] Currently, there are no reports of isatins reacting with biological amines. Thus, the reactivity between AIR and isatin appears to be novel. Such a result highlights the unique reactivity of AIR that is likely important for the carboxylation of AIR to produce CAIR in *de novo* purine biosynthesis. The chemical structure of the product formed by the reaction between AIR and isatin is currently under investigation, and that report is forthcoming.

Isatins have been reported in the literature to possess cytotoxic effects across a range of microorganisms and various cancer cell lines.[31–57] The mechanism of cytotoxic action of isatins is unknown, and it is tempting to speculate that one mechanism of cytotoxicity is due to the depletion of AIR resulting in the inhibition of purine biosynthesis. While plausible, the reactivity of isatins with biological sulfhydryl groups complicates the determination of the effect of isatin on purine biosynthesis. The use of substrate depletion as a mechanism to inhibit bacterial growth is intriguing because it would presumably be difficult for bacteria to

develop resistance to such a mechanism. Vancomycin, a currently used antibiotic, can be thought of as working via a substrate depletion mechanism because it binds to the substrate, thus preventing it from reacting with the enzyme. Resistance to vancomycin took more than 20 years to be observed in the clinic, attesting to the challenge of bacteria developing resistance to a substrate depletion drug. Unfortunately, AIR is an intermediate of *de novo* purine biosynthesis for bacteria and humans. Therefore, substrate depletion of AIR by isatin does not provide the selectivity required to be utilized as an antibacterial agent.

Acknowledgments

Funding

The authors thank the National Institute of General Medical Sciences (S.M.F., GM087467) and the American Foundation for Pharmaceutical Education (CCS) for financial support.

REFERENCES

(1). Coates AR, Halls G, and Hu Y (2011) Novel classes of antibiotics or more of the same? Br. J. Pharmacol 163 (1), 184–94. [PubMed: 21323894]

(2). Chen ZD, Dixon JE, and Zalkin H (1990) Cloning of a chicken liver cDNA encoding 5-aminoimidazole ribonucleotide carboxylase and 5-aminoimidazole-4-N-succinocarboxamide ribonucleotide synthetase by functional complementation of Escherichia coli pur mutants. Proc. Natl. Acad. Sci. U. S. A 87 (8), 3097–101. [PubMed: 1691501]

(3). Watanabe W, et al. (1989) Identification and sequence analysis of Escherichia coli purE and purK genes encoding 5′-phosphoribosyl-5-amino-4-imidazole carboxylase for de novo purine biosynthesis. J. Bacteriol 171 (1), 198–204. [PubMed: 2644189]

(4). Meyer E, et al. (1992) Purification and characterization of the purE, purK, and purC gene products: identification of a previously unrecognized energy requirement in the purine biosynthetic pathway. Biochemistry 31 (21), 5022–32. [PubMed: 1534690]

(5). Thoden JB, et al. (1999) Three-dimensional structure of N5-carboxyaminoimidazole ribonucleotide synthetase: a member of the ATP grasp protein superfamily. Biochemistry 38 (47), 15480–92.

(6). Meyer E, et al. (1999) Evidence for the direct transfer of the carboxylate of N5-carboxyaminoimidazole ribonucleotide (N5-CAIR) to generate 4-carboxy-5-aminoimidazole ribonucleotide catalyzed by Escherichia coli PurE, an N5-CAIR mutase. Biochemistry 38 (10), 3012–8. [PubMed: 10074353]

(7). Crawford RM, et al. (1996) Deletion of purE attenuates Brucella melitensis infection in mice. Infect. Immun 64 (6), 2188–92. [PubMed: 8675325]

(8). Flashner Y, et al. (2004) Generation of Yersinia pestis attenuated strains by signature-tagged mutagenesis in search of novel vaccine candidates. Infect. Immun 72 (2), 908–15. [PubMed: 14742535]

(9). Kirsch DR, and Whitney RR (1991) Pathogenicity of Candida albicans auxotrophic mutants in experimental infections. Infect. Immun 59 (9), 3297–300. [PubMed: 1879944]

(10). Lan L, et al. (2010) Golden pigment production and virulence gene expression are affected by metabolisms in Staphylococcus aureus. J. Bacteriol 192 (12), 3068–77. [PubMed: 20400547]

(11). Polissi A, et al. (1998) Large-scale identification of virulence genes from Streptococcus pneumoniae. Infect. Immun 66 (12), 5620–9. [PubMed: 9826334]

(12). Samant S, et al. (2008) Nucleotide biosynthesis is critical for growth of bacteria in human blood. PLoS Pathog. 4 (2), No. e37.

(13). Firestine SM, et al. (2009) Identification of inhibitors of N5-carboxyaminoimidazole ribonucleotide synthetase by high-throughput screening. Bioorg. Med. Chem 17 (9), 3317–23. [PubMed: 19362848]

(14). Dewal MB, and Firestine SM (2013) Site-directed mutagenesis of catalytic residues in N(5)-carboxyaminoimidazole ribonucleotide synthetase. Biochemistry 52 (37), 6559–67. [PubMed: 23899325]

(15). Firestine SM, and Davisson VJ (1994) Carboxylases in de novo purine biosynthesis. Characterization of the Gallus gallus bifunctional enzyme. Biochemistry 33 (39), 11917–26.

(16). Meyer E, et al. (1992) Purification and Characterization of the Pure, Purk, and Purc Gene-Products - Identification of a Previously Unrecognized Energy Requirement in the Purine Biosynthetic-Pathway. Biochemistry 31 (21), 5022–5032. [PubMed: 1534690]

(17). Casey PJ, and Lowenstein JM (1987) Inhibition of adenylosuccinate lyase by L-alanosyl-5-aminoimidazole-4-carboxylic acid ribonucleotide (alanosyl-AICOR). Biochem. Pharmacol 36 (5), 705–9. [PubMed: 3827951]

(18). Reiner JM (1959) Behavior of enzyme systems; an analysis of kinetics and mechanism, pp 148–162, Burgess Publishing Co., Minneapolis, MN.

(19). Oliviero G, et al. (2010) Facile Solid-Phase Synthesis of AICAR 5 ‘-Monophosphate (ZMP) and Its 4-N-Alkyl Derivatives. Eur. J. Org. Chem 2010 (8), 1517–1524.

(20). Mahal A, et al. (2015) Synthesis of cyclic N1-pentylinosine phosphate, a new structurally reduced cADPR analogue with calciummobilizing activity on PC12 cells. Beilstein J. Org. Chem 11, 2689–2695. [PubMed: 26877790]

(21). Oliviero G, et al. (2007) Synthesis of N-1 and ribose modified inosine analogues on solid support. Tetrahedron Lett. 48 (3), 397–400.

(22). Kohyama N, and Yamamoto Y (2003) A facile synthesis of AICAR from inosine. Synthesis No. 17, 2639–2642.

(23). Firestine SM, et al. (2009) Interrogating the mechanism of a tight binding inhibitor of AIR carboxylase. Bioorg. Med. Chem 17 (2), 794–803. [PubMed: 19095456]

(24). Firestine SM, and Davisson VJ (1994) Carboxylases in De-Novo Purine Biosynthesis - Characterization of the Gallus-Gallus Bifunctional Enzyme. Biochemistry 33 (39), 11917–11926.

(25). Groziak MP, et al. (1997) Effect of a chemical modification on the hydrated adenosine intermediate produced by adenosine deaminase and a model reaction for a potential mechanism of action of 5-aminoimidazole ribonucleotide carboxylase. J. Med. Chem 40 (21), 3336–3345. [PubMed: 9341908]

(26). Di Carlo FJ, and Lindwall HG (1945) Synthesis and Properties of 1-Cyanoethylisatin. J. Am. Chem. Soc 67 (2), 199–201.

(27). Baell JB, and Holloway GA (2010) New substructure filters for removal of pan assay interference compounds (PAINS) from screening libraries and for their exclusion in bioassays. J. Med. Chem 53 (7), 2719–40. [PubMed: 20131845]

(28). Yang JJ, et al. (2016) Badapple: promiscuity patterns from noisy evidence. J. Cheminf 8, 29.

(29). Nissin JWM, and Blackbur S. (2014) Quantification of frequent-hitter behavior based on historical high-throughput screening data. Future Med. Chem 6 (10), 1113–1126. [PubMed: 25078133]

(30). Lee D, et al. (2000) Potent and selective nonpeptide inhibitors of caspases 3 and 7 inhibit apoptosis and maintain cell functionality. J. Biol. Chem 275 (21), 16007–14.

(31). Varma RS, and Nobles WL (1975) Antiviral, antibacterial, and antifungal activities of isatin N-Mannich bases. J. Pharm. Sci 64 (5), 881–2. [PubMed: 1151666]

(32). Maysinger D, Ban J, and Movrin M (1980) Effects of isatin N-Mannich bases on HeLa cells. Arzneimittelforschung 30 (6), 932–5. [PubMed: 7191266]

(33). Maysinger D, Movrin M, and Saric MM (1980) Structural analogues of isatin and their antimicrobial activity. Pharmazie 35 (1), 14–6. [PubMed: 7384170]

(34). Cane A, et al. (2000) The endogenous oxindoles 5-hydroxyoxindole and isatin are antiproliferative and proapoptotic. Biochem. Biophys. Res. Commun 276 (1), 379–84. [PubMed: 11006132]

(35). Igosheva N, et al. (2005) Isatin, an endogenous monoamine oxidase inhibitor, triggers a dose- and time-dependent switch from apoptosis to necrosis in human neuroblastoma cells. Neurochem. Int 47 (3), 216–24. [PubMed: 15876476]

(36). Vine KL, et al. (2007) In vitro cytotoxicity evaluation of some substituted isatin derivatives. Bioorg. Med. Chem 15 (2), 931–8. [PubMed: 17088067]

(37). Vine KL, et al. (2007) An investigation into the cytotoxicity and mode of action of some novel N-alkyl-substituted isatins. J. Med. Chem 50 (21), 5109–17. [PubMed: 17887662]

(38). Hou L, et al. (2008) Antitumor effects of Isatin on human neuroblastoma cell line (SH-SY5Y) and the related mechanism. Eur. J. Pharmacol 589 (1–3), 27–31. [PubMed: 18561913]

(39). Matesic L, et al. (2008) N-phenethyl and N-naphthylmethyl isatins and analogues as in vitro cytotoxic agents. Bioorg. Med. Chem 16 (6), 3118–24. [PubMed: 18182300]

(40). Krishnegowda G, et al. (2011) Synthesis and biological evaluation of a novel class of isatin analogs as dual inhibitors of tubulin polymerization and Akt pathway. Bioorg. Med. Chem 19 (20), 6006–14. [PubMed: 21920762]

(41). Chen G, et al. (2012) New bactericide derived from Isatin for treating oilfield reinjection water. Chem. Cent. J 6 (1), 90. [PubMed: 22929650]

(42). Edwards V, Benkendorff K, and Young F (2012) Marine compounds selectively induce apoptosis in female reproductive cancer cells but not in primary-derived human reproductive granulosa cells. Mar. Drugs 10 (1), 64–83. [PubMed: 22363221]

(43). Premanathan M, et al. (2012) Antioxidant & anticancer activities of isatin (1H-indole-2,3-dione), isolated from the flowers of Couroupita guianensis Aubl. Indian J. Med. Res 136 (5), 822–6. [PubMed: 23287130]

(44). Singh P, et al. (2012) Azide-alkyne cycloaddition en route to novel 1H-1,2,3-triazole tethered isatin conjugates with in vitro cytotoxic evaluation. Eur. J. Med. Chem 55, 455–61. [PubMed: 22818042]

(45). Vine KL, et al. (2012) Targeting urokinase and the transferrin receptor with novel, anti-mitotic N-alkylisatin cytotoxin conjugates causes selective cancer cell death and reduces tumor growth. Curr. Cancer Drug Targets 12 (1), 64–73. [PubMed: 22111834]

(46). Chiang YR, et al. (2013) An in vitro study of the antimicrobial effects of indigo naturalis prepared from Strobilanthes formosanus Moore. Molecules 18 (11), 14381–96. [PubMed: 24284490]

(47). Raj R, et al. (2013) Synthesis of 1H-1,2,3-triazole linked betalactam-isatin bi-functional hybrids and preliminary analysis of in vitro activity against the protozoal parasite Trichomonas vaginalis. Eur. J. Med. Chem 63, 897–906. [PubMed: 23631874]

(48). Reddy SS, et al. (2013) Synthesis and evaluation of the cytotoxic activities of some isatin derivatives. Chem. Pharm. Bull 61 (11), 1105–13. [PubMed: 24005772]

(49). Song J, et al. (2013) Isatin inhibits proliferation and induces apoptosis of SH-SY5Y neuroblastoma cells in vitro and in vivo. Eur. J. Pharmacol 702 (1–3), 235–41. [PubMed: 23376416]

(50). Esmaeelian B, et al. (2014) 6-bromoisatin found in muricid mollusc extracts inhibits colon cancer cell proliferation and induces apoptosis, preventing early stage tumor formation in a colorectal cancer rodent model. Mar. Drugs 12 (1), 17–35.

(51). Han K, et al. (2014) Design, synthesis and in vitro cytotoxicity evaluation of 5-(2-carboxyethenyl)isatin derivatives as anticancer agents. Bioorg. Med. Chem. Lett 24 (2), 591–4. [PubMed: 24360564]

(52). Li Z, et al. (2014) A freshwater bacterial strain, Shewanella sp. Lzh-2, isolated from Lake Taihu and its two algicidal active substances, hexahydropyrrolo[1,2-a]pyrazine-1,4-dione and 2, 3-indolinedione. Appl. Microbiol. Biotechnol 98 (10), 4737–48. [PubMed: 24566920]

(53). Ma Z, et al. (2014) The endogenous oxindole isatin induces apoptosis of MCF7 breast cancer cells through a mitochondrial pathway. Oncol. Rep 32 (5), 2111–7. [PubMed: 25174967]

(54). Zhou Y, et al. (2014) 5-(2-carboxyethenyl) isatin derivative induces G(2)/M cell cycle arrest and apoptosis in human leukemia K562 cells. Biochem. Biophys. Res. Commun 450 (4), 1650–5. [PubMed: 25044115]

(55). Sharma S, et al. (2015) Triazole linked mono carbonyl curcumin-isatin bifunctional hybrids as novel anti tubulin agents: Design, synthesis, biological evaluation and molecular modeling studies. Bioorg. Med. Chem 23 (22), 7165–80. [PubMed: 26515041]

(56). Wu C, et al. (2015) Metabolomics-Driven Discovery of a Prenylated Isatin Antibiotic Produced by Streptomyces Species MBT28. J. Nat. Prod 78 (10), 2355–63. [PubMed: 26438963]

(57). Gil-Turnes MS, Hay ME, and Fenical W (1989) Symbiotic marine bacteria chemically defend crustacean embryos from a pathogenic fungus. Science 246 (4926), 116–8. [PubMed: 2781297]

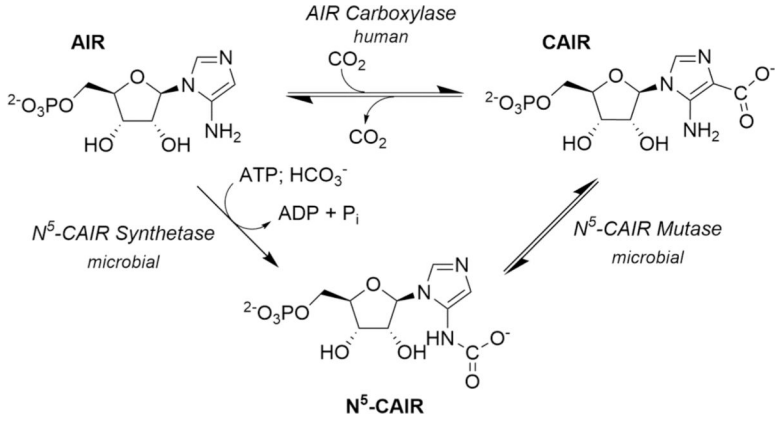

Figure 1.

Divergence in the *de novo* purine biosynthetic pathway. Humans convert AIR to CAIR using the enzyme AIR carboxylase with CO_2 as the one-carbon source (top). Microbes convert AIR to N^5-CAIR using the enzyme N^5-CAIR synthetase and HCO_3^- as the one-carbon source along with ATP. The conversion of N^5-CAIR to CAIR is conducted by the enzyme N^5-CAIR mutase (bottom).

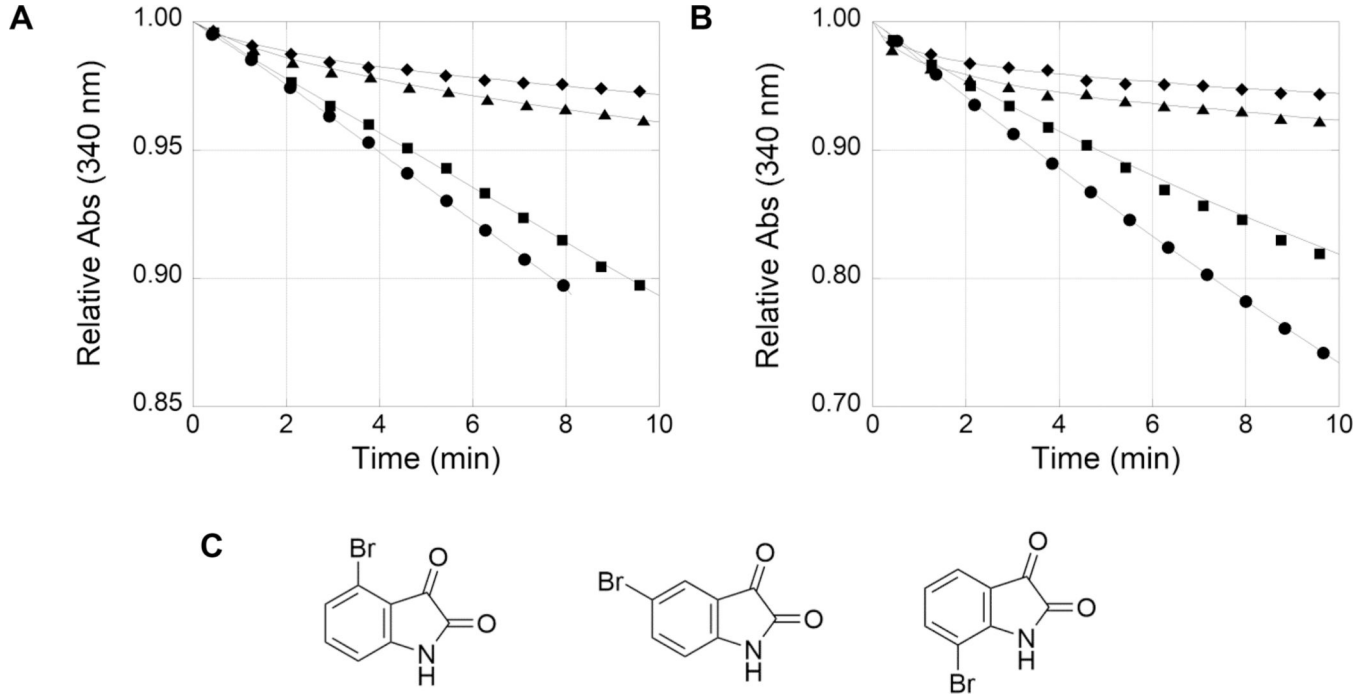

Figure 2.

Inhibition of N^5-CAIR synthetase by isatin in the ATP-NADH coupled assay. The ATP-NADH coupled N^5-CAIR synthetase reaction was initiated with AIR (25 μM) and bromoisatin (100 μM) at time zero, and the conversion of NADH to NAD^+ was measured at 340 nm. Seventy nanograms of the *A. clavatus* enzyme (A) or 110 ng of the *E. coli* enzyme (B) was used in the assay. (C) 4-Bromo-, 5-bromo-, and 7-bromoisatin from left to right, respectively. Legend: no isatin (●), 4-bromoisatin (■), 7-bromoisatin (▲), and 5-bromoisatin (◆). The *Y*-axes have different scales, from 0.85 to 1.00 for panel A and from 0.70 to 1.00 for panel B. The lines in all graphs are the best-fit lines as executed by KaleidaGraph. The experiments generated continuous data; however, only a limited number of data points for each curve are shown for the sake of clarity.

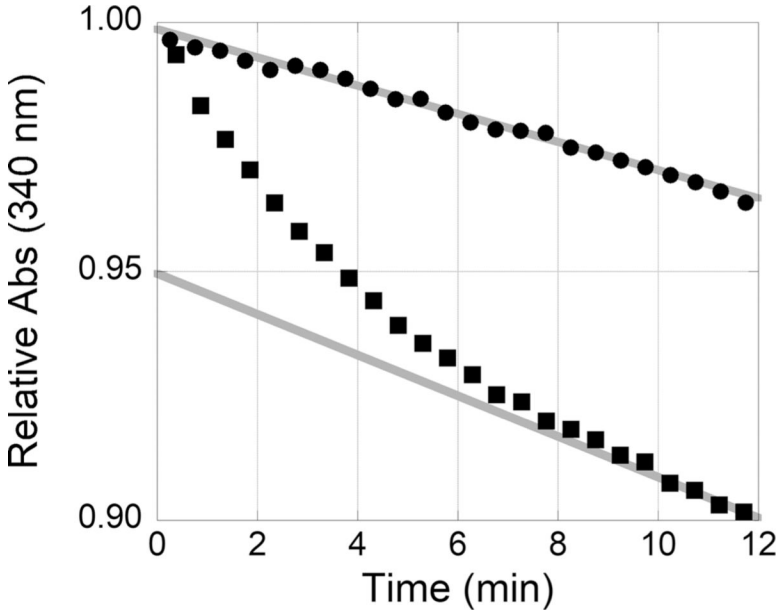

Figure 3.

The order of addition is important between the reaction of isatin and AIR. Left: 1-Methylisatin. Right: *A. clavatus* N^5-CAIR synthetase ATP-NADH coupled assay with 200 μM 1-methylisatin incubated with AIR and initiated with the enzyme (●) or 200 μM 1-methylisatin incubated with the enzyme and initiated with AIR (■). The steady-state rates for initiation with the enzyme (−0.003 OD/min) or AIR (−0.004 OD/min) are colored gray. The steady-state rate for the initiation of AIR was determined from data from 10 to 12 min. The data in the graph are 24 evenly selected points from a continuous data set from 0 to 12 min.

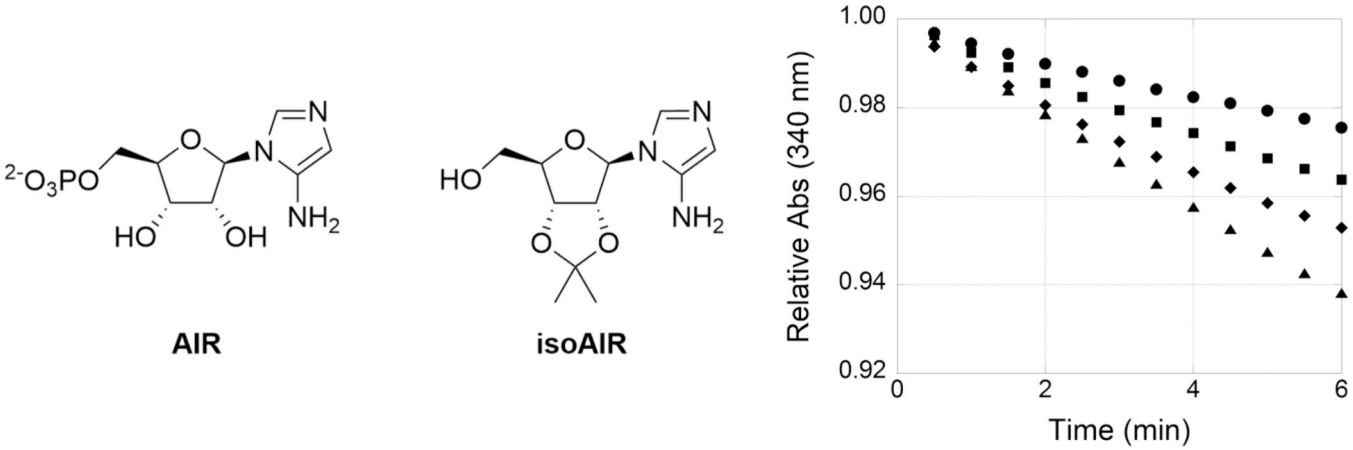

Figure 4.

Structures of AIR and isoAIR and the effect that isoAIR has on the inhibition of N^5-CAIR synthetase. Structures of AIR and isoAIR (left). *A. clavatus* N^5-CAIR synthetase ATP-NADH coupled assay with 200 μM 1-methylisatin with the addition of various concentrations of isoAIR (right). Legend: 0 (●), 200 (■), 400 (◆), and 800 μM (▲) isoAIR.

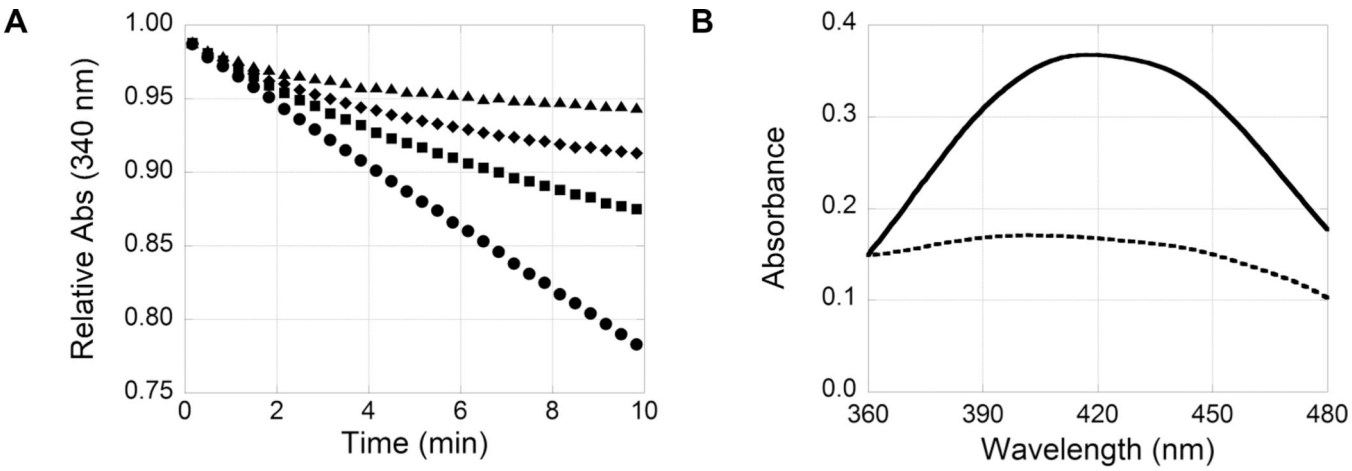

Figure 5.

(A) Dose-dependent inhibition of N^5-CAIR synthetase. ATP-NADH coupled assay with 0 (●), 50 (■), 100 (◆), and 200 μM (▲) 1-methylisatin. (B) Monitoring AIR:isatin product formation at 420 nm. UV–vis scan of the reaction of 500 μM 1-methylisatin with 1200 μM AIR at 0 (—) and 5 min (---).

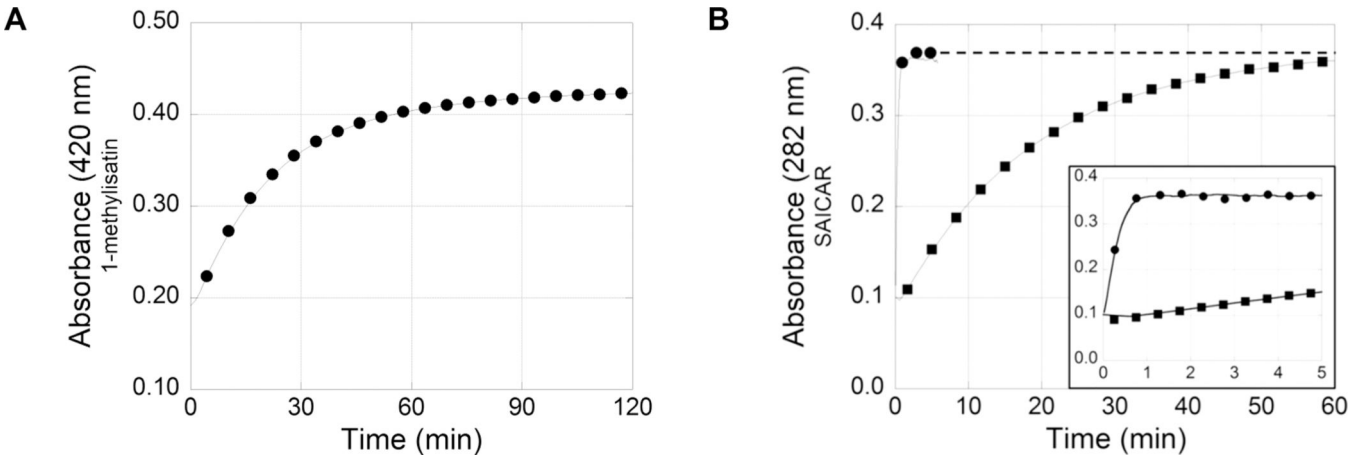

Figure 6.

Reversibility of 1-methylisatin and AIR reactions via the SAICAR synthetase coupled assay. (A) 1-Methylisatin (500 μM) incubated with excess AIR coupled to the enzymes necessary to convert AIR into the irreversible product SAICAR (Scheme 3). The conversion of the product to the starting material, 1-methylisatin, was monitored by UV–vis at 420 nm. (B) Production of SAICAR from 50 μM AIR was monitored by UV–vis at 282 nm without 1-methylisatin (●) and with 200 μM 1-methylisatin (■). The inset displays the first 5 min of the reaction.

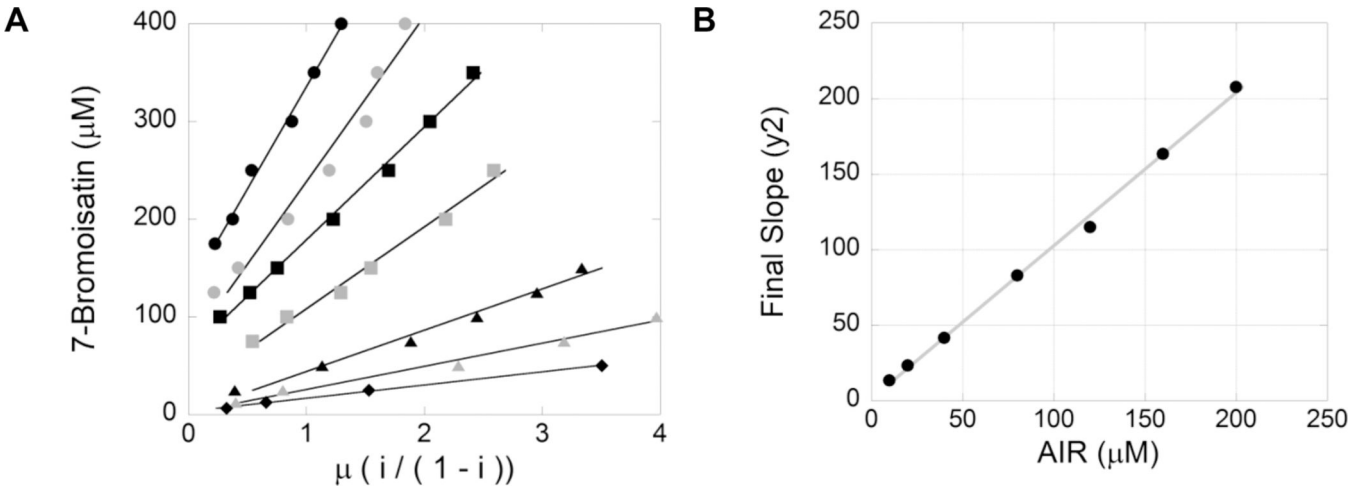

Figure 7.

Determination of the substrate depletion mechanism. (A) Plot of inhibitor, 7-bromoisatin (μM), vs μ, fractional inhibition, of the ATP-NADH coupled assay with various concentrations of AIR: 200 (black circles), 160 (gray circles), 120 (black squares), 80 (gray squares), 40 (black triangles), 20 (gray triangles), and 10 μM (black diamonds) from top to bottom, respectively. (B) Plot of the final slope (y_2) from panel A vs AIR (μM).

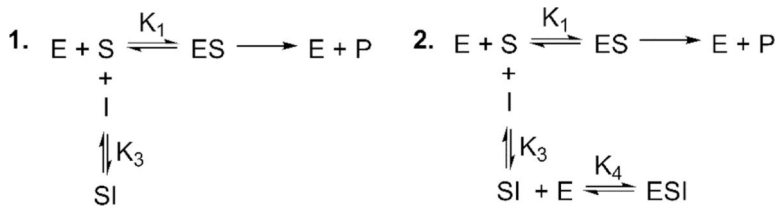

Scheme 1.

Two Mechanisms for Inhibition of an Enzyme by an Inhibitor:Substrate Complex[a]

[a]Mechanism 1 is inhibition by pure substrate depletion. Mechanism 2 is inhibition by substrate depletion and inhibition of the enzyme by the inhibitor:substrate complex.

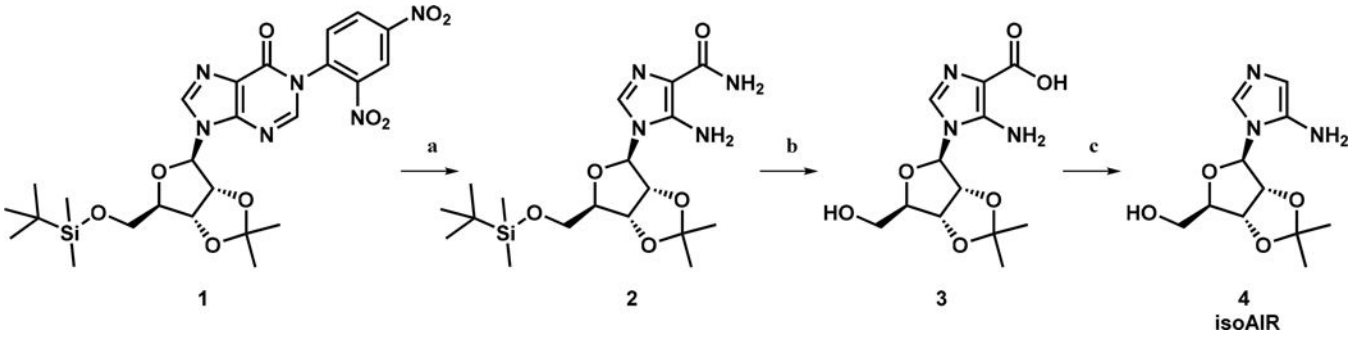

Scheme 2.

Synthesis of IsoAIR[a]

[a]Reagents and conditions: (a) ethylenediamine, dimethylformamide, 50 °C, 4 h, 68%; (b) 6 N NaOH, reflux, 5 h, 83%; (c) NH_4OAc, 20 mM, pH 4.8, room temperature, 7 h, 70%.

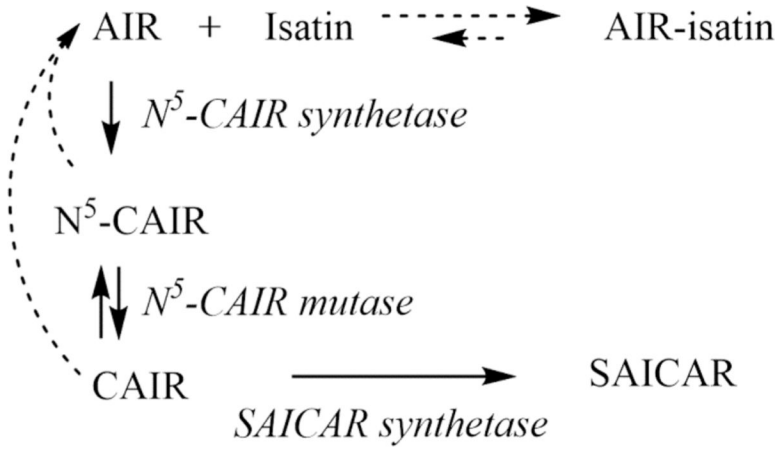

Scheme 3.

Coupled Enzymatic Assay System for Converting N^5-CAIR into SAICAR[a]

[a]The solid arrows represent enzymatic reactions, while the dashed arrows represent non-enzymatic reactions.